Energy Conversion and Management: X 30 (2026) 101579

Contents lists available at ScienceDirect

Energy Conversion and Management: X

journal homepage: www.sciencedirect.com/journal/energy-conversion-and-management-x

Economic dispatch optimization of a metal hydride storage system for supplying heat and electricity in a residential application

Carlos Muñoz [a], Nies Reininghaus [a], Julián Puszkiel [b,c,*], Astrid Pistoor [a], Michael Kroener [a], Alexander Dyck [a], Martin Vehse [a], Thomas Klassen [b,c], Julian Jepsen [b,c]

[a] Institute of Networked Energy Systems, German Aerospace Center (DLR), Carl-von-Ossietzky-Straße 15, Oldenburg, 26129, Lower Saxony, Germany
[b] Institute of Hydrogen Technology, Helmholtz-Zentrum Hereon, Max–Planck-Straße 1, Geesthacht, 21502, Schleswig-Holstein, Germany
[c] Institute of Materials Science, Helmut-Schmidt University, University of the Federal Armed Forces Hamburg, Holstenhofweg 85, Hamburg, 22043, Hamburg, Germany

ARTICLE INFO

Keywords:
Metal hydride
Economic dispatch
System modeling
Optimization
Sector integration
Cost minimization
Household

ABSTRACT

To achieve affordable, clean energy, incorporating renewable energy into existing energy systems is the key. One challenge is the fluctuating nature of renewable resources, which can be asynchronous with energy demands. Hydrogen storage, particularly metal hydride storage, is a favorable solution for balancing supply and demand. In particular, metal hydride storage, compared with pressurized or liquefied hydrogen storage, is a favorable technology choice due to its storage energy density (50-100 kg H_2/m^3) and its low operating temperature and pressure. This paper presents a simulation-based framework to investigate the optimal design and operation of a coupled Electrolyzer-Fuel Cell-Metal Hydride system (SET-Unit) for minimizing operational and capital expenses in a residential application. The results show that integrating heat pumps with a metal-hydride storage system and photovoltaics can achieve 83% energy self-sufficiency and a 7.1-year payback period. Combining SET-Unit, gas boilers, and photovoltaics can result in 28% energy self-sufficiency, annual savings of over 2221 EUR, and a payback period of 7.4 years. The SET-Unit, combined with renewable energy sources such as photovoltaics, and the in-market available gas boilers or heat pumps, shows benefits in efficiency, annual energy cost reduction, and a relatively short payback period for the household. Using the low end of published values for capital expenses, economic feasibility can be achieved.

1. Introduction

The existing climate change and its current effects on our planet [1], and the inevitable increase in global energy consumption due to the expected population growth by approximately 1.7 billion by 2050 [2], are significant challenges we face today. To address such challenges, several countries have pushed for the use of renewable energy sources, in line with Sustainable Development Goal 7 (SDG7) [3,4]. More precisely, the share of renewable energy sources in the global final electricity consumption was significant in 2021, reaching 28.2% [5]. However, a critical issue with renewable energy sources, particularly wind and solar, is their high fluctuation and uncertainty, leading to unstable electricity output [1,3].

An efficient method to overcome the fluctuations and uncertainties of renewable energy sources is the use of energy storage systems [6], which typically charge during periods of low energy demand and discharge during periods of high energy demand [7]. In the energy storage field, hydrogen storage is currently at the forefront of research, as it is considered a necessary component of the present and future energy systems [8]. An important benefit of a hydrogen storage system coupled with renewable energy sources and a consumer (e.g., residential, commercial, industrial) is the balancing of fluctuations in both energy production [9] and energy demand [10], even when production and demand do not occur simultaneously. However, storing hydrogen poses some challenges, mainly due to its low volumetric energy density: as a gas, it is only 0.003 kWh/L at 1 atm and 0 °C [11].

Metal hydride (MH) storage offers an advantageous solution for significantly increasing the volumetric energy density of hydrogen. The storage of hydrogen as a metal hydride allows operation at low pressures, down to 10 bar, operating temperatures near ambient, achieving up to two times the cryogenic volumetric density within the storage

* Corresponding author at: Institute of Hydrogen Technology, Helmholtz-Zentrum Hereon, Max–Planck-Straße 1, Geesthacht, 21502, Schleswig-Holstein, Germany.
E-mail addresses: charlesmr1094@gmail.com (C. Muñoz), julian.puszkiel@hereon.de (J. Puszkiel).

https://doi.org/10.1016/j.ecmx.2026.101579
Received 4 June 2025; Received in revised form 23 December 2025; Accepted 15 January 2026
Available online 21 January 2026

Nomenclature

C	Total energy cost for a year (EUR)
$CAPEX$	Capital expenses (EUR)
gb	Gas boiler
hp	Heat pump
P_{elec}	Electricity price (EUR/kWh)
P_{gas}	Gas price (EUR/kWh)
PP	Payback Period (years)
ref	Reference case
S	Savings (EUR)
set	Case with SET-Unit
SS	Self-sufficiency ratio
H_2	Hydrogen
kW_p	Kilowatt peak
BC	Boundary conditions
COP	Coefficient of Performance
Digi-HyPro	Digitalized Hydrogen Process Chain for the Energy Transition
DWD	Deutscher Wetterdienst
EL	Electrolyzer
ELP	Electric load profile
ESM	Energy system model
FC	Fuel cell
HLP	Heat load profile
MH	Metal hydride
PtGtP	Power-to-Gas-to-Power
PV	Photovoltaic
SET-Unit	Smart-Energy-Transform-Unit
SFH	Single-Family house
TS	Thermal Storage

material and four times the compressed hydrogen at 700 bar, and enabling safe operation [12–14].

MH storage has been identified as an excellent choice for a Power-to-Gas-to-Power (PtGtP) system, typically composed of an electrolyzer (EL), a fuel cell (FC), a renewable energy source such as photovoltaic (PV) or wind, and a sink (e.g., a consumer) [15–27]. A study of different hydrogen storage choices in a PtGtP system for residential heating revealed that the MH storage system provides excellent performance in the areas of safety, energy density, durability, and kinetics (rate of reactions) [23].

In the literature review of PtGtP systems with MH storage, a research gap was identified in the operation and component dimensioning for supplying both electrical and thermal demands, thereby minimizing costs for residential applications, i.e., SFH (single-family house). To close this research gap, this paper develops a simulation-based framework to investigate the design and operation of the SET-Unit (Smart Energy Transition Unit) of the Digi-HyPro project at minimum cost, i.e., minimum operational and capital expenses [24–27]. A key benefit of the SET-Unit is its ability to supply not only electricity but also heat, which is required in a household, making it a good match for simultaneous electricity and heat residential loads. For this reason, a residential use case has been selected as an application of the simulation model. This use case is shown in Fig. 1.

When electricity from a residential rooftop solar photovoltaic (PV) system is available, the electrolyzer generates hydrogen, which is then stored in the MH storage. Hydrogen can be fed to a fuel cell to generate electricity to meet the SFH's electrical demands. Electric demand can also be met by either additional excess generation from the PV system or by importing electricity from the grid at a certain cost. Excess electricity from the PV system can be sold to the power grid at a fixed feed-in tariff. In addition, waste heat from the electrolyzer, the fuel cell, and hydrogen storage can be used to meet part of the building's heat demand. Moreover, an electrical heat pump and thermal storage can provide heat and store it in water, respectively, as shown in Fig. 1. Alternatively, a gas boiler can serve as a heating device for an SFH.

2. Methods

The overall method followed in this paper can be seen in Fig. 2. Four general steps are followed: definition of households and cases, energy system model and optimization, definition of boundary conditions (BC), and comparison of each result. The following sections explain each general step of the method in detail.

2.1. Cases of study: Application of the methodology to a single-family house (SFH)

For the application of the method, two typical SFHs in Germany were initially defined for the cases of study with respect to electricity and heat demand. The analysis employs German SFH demand profiles due to their high data quality, regulatory relevance, and technological representativeness within the EU context [28]. A 3-person household is assumed as it reflects a statistically significant [29] and energy-efficient household size across Europe, optimizing system design and economic feasibility. While the results demonstrate strong generalizability potential — particularly for countries with similar building stocks, heating demands, and policy frameworks — limitations include geographical specificity, climate variations, and uncertainties in technology costs and long-term performance. Future work should validate findings across diverse EU regions and household types to ensure broader applicability. As the total share of heat pumps in single and multi-family houses is increasing, i.e., 5.3% in 2023 vs. 3.4% in 2019 [30], a heat pump was assumed as the heating device in the first SFH. Stratified thermal storage (TS) was also assumed to be present in the first SFH. Both houses were connected to the electrical grid (as seen in Fig. 1) in case grid import was needed. In the second SFH, the heating device assumed was the gas boiler, as it represented around 40% of the heating devices in single and multi-family houses in 2023 [30]. The electrical grid and the gas grid were available to the house in case electricity import or gas import was required, respectively.

For each SFH, two cases were defined: (a) a reference case, where the members of the house did not invest into the SET-Unit but rather performed economic dispatch of the electricity and heat demand of the house based on its initial components, and (b) a case with SET-Unit, where economic dispatch was performed based on the initial components of the house and SET-Unit components.

2.2. Energy System Model (ESM)

To operate the devices of the reference case and with the SET-Unit case with the aim of minimizing costs, i.e., economic dispatch, the open energy modeling framework (oemof) was used [31,32]. The oemof is a Python package that can be used to model energy systems and perform dispatch optimization to minimize costs. Diverse publications have used oemof, including the modeling of an energy system interacting with energy components of a refrigerated trailer [33], and the analysis of the provision of electricity and heat to buildings with a fuel cell electric vehicle [34].

The energy system model in oemof that was built for the reference case and the case with SET-Unit for both SFH can be seen in Fig. 3. Two type of nodes can be used in oemof: buses and components. A component can further be classified as sink, source, transformer or generic storage. The electric demand and the heat demand of both SFH study cases were modeled as sinks. In each SFH, the grid import and the gas import were modeled as sources. The electric heat pump and the gas

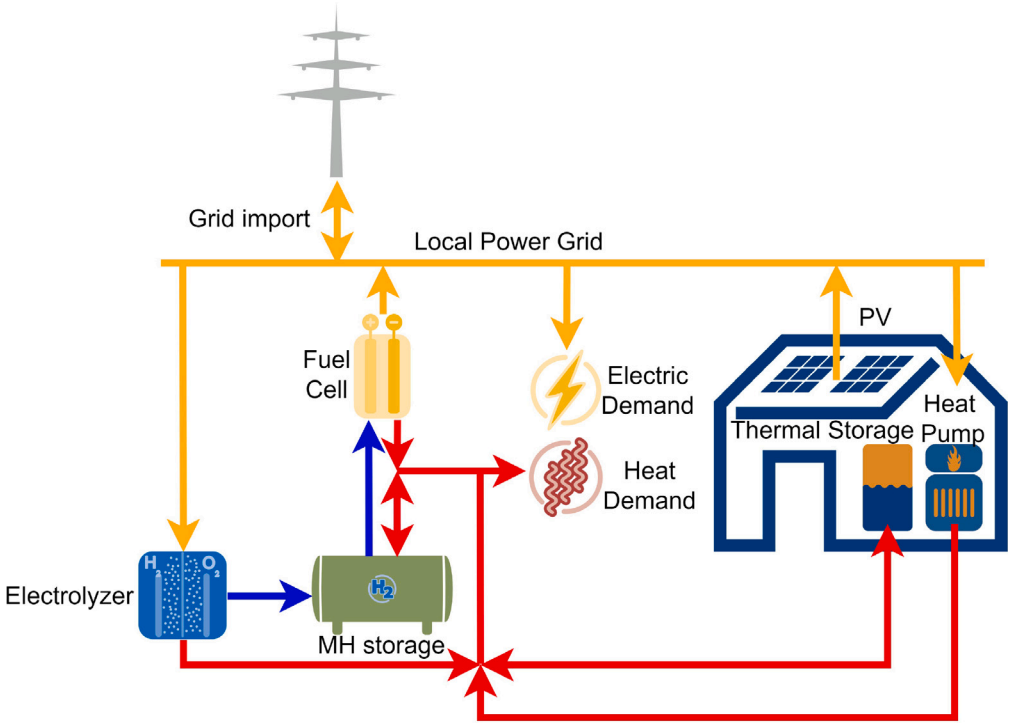

Fig. 1. SET-Unit providing electricity and heat demands for a residential application. The electricity flow (orange), hydrogen flow (blue), and heat flow (red) are depicted with arrows. (For interpretation of the references to colour in this figure legend, the reader is referred to the web version of this article.)

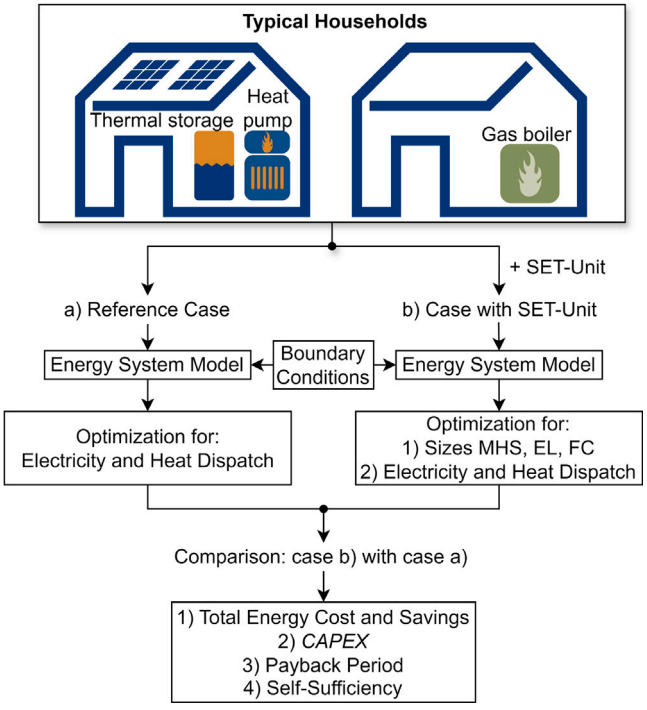

Fig. 2. Method applied in this article. MHS: metal hydride storage; EL: electrolyzer; FC: fuel cell; $CAPEX$: capital expenses.

boiler were employed as transformers in each respective SFH, as each one converts from one type of energy to another type. The heat pump converts electrical energy to thermal energy with a factor represented by the COP, while the gas boiler burns gas to produce heat, considering the efficiency of the device. The thermal storage was used as a generic storage. An electricity bus, a heat bus, and a gas bus were used as well. The flow of energy is depicted with arrows, which always connect a bus with a component. The reference case for the SFH with heat pump excludes the SET-Unit, while the reference case for the SFH with gas boiler excludes the PV system source, excess electricity sink, and the SET-Unit.

For the case with SET-Unit, all nodes depicted in Fig. 3 are included. The electrolyzer and the fuel cell devices were modeled as transformers and each device released heat to the heat bus. The heat flow from the MH absorption process was modeled by using the transformer MH absorption where the heat is flowing to the heat bus. On the other hand, the heat flow from the MH desorption process goes from the heat bus to the MH desorption transformer. The heat flow during MH absorption was assumed to be 21.5 kJ/mol H_2, while for the MH desorption the value used was 31.79 kJ/mol H_2. These values correspond to the enthalpies of reaction for the MH absorption and desorption of hydride forming alloys [35]. These values were then converted to the units of kWh-heat per kWh of hydrogen, as the energy flows in oemof are in the units of kWh for every hour. Using the low heating value of hydrogen, the heat flow value used for MH absorption in oemof was: $21.5\ \frac{\text{kJ}}{\text{mol H}_2} \cdot \frac{1\ \text{mol H}_2}{2\ \text{g H}_2} \cdot \frac{1000\ \text{g}}{1\ \text{kg}} \cdot \frac{1\ \text{kWh}}{3600\ \text{kJ}} \cdot \frac{1\ \text{kg H}_2}{33.33\ \text{kWh H}_2} = 0.0896$ kWh-heat per kWh of H_2 stored, while the value used for MH desorption was: $31.79\ \frac{\text{kJ}}{\text{mol H}_2} \cdot \frac{1\ \text{mol H}_2}{2\ \text{g H}_2} \cdot \frac{1000\ \text{g}}{1\ \text{kg}} \cdot \frac{1\ \text{kWh}}{3600\ \text{kJ}} \cdot \frac{1\ \text{kg H}_2}{33.33\ \text{kWh H}_2} = 0.13248$ kWh-heat per kWh of H_2 released. The MH storage was employed as a generic storage. The PV system was used as a source, and excess electricity from the PV system was used as a sink. Hydrogen buses were employed similarly.

The parameters assumed for each component of Fig. 3 and boundary conditions assumed for the energy system models are described in the following section.

2.3. Boundary Conditions (BC)

In this section, the assumptions and parameters assumed for the ESM will be explained.

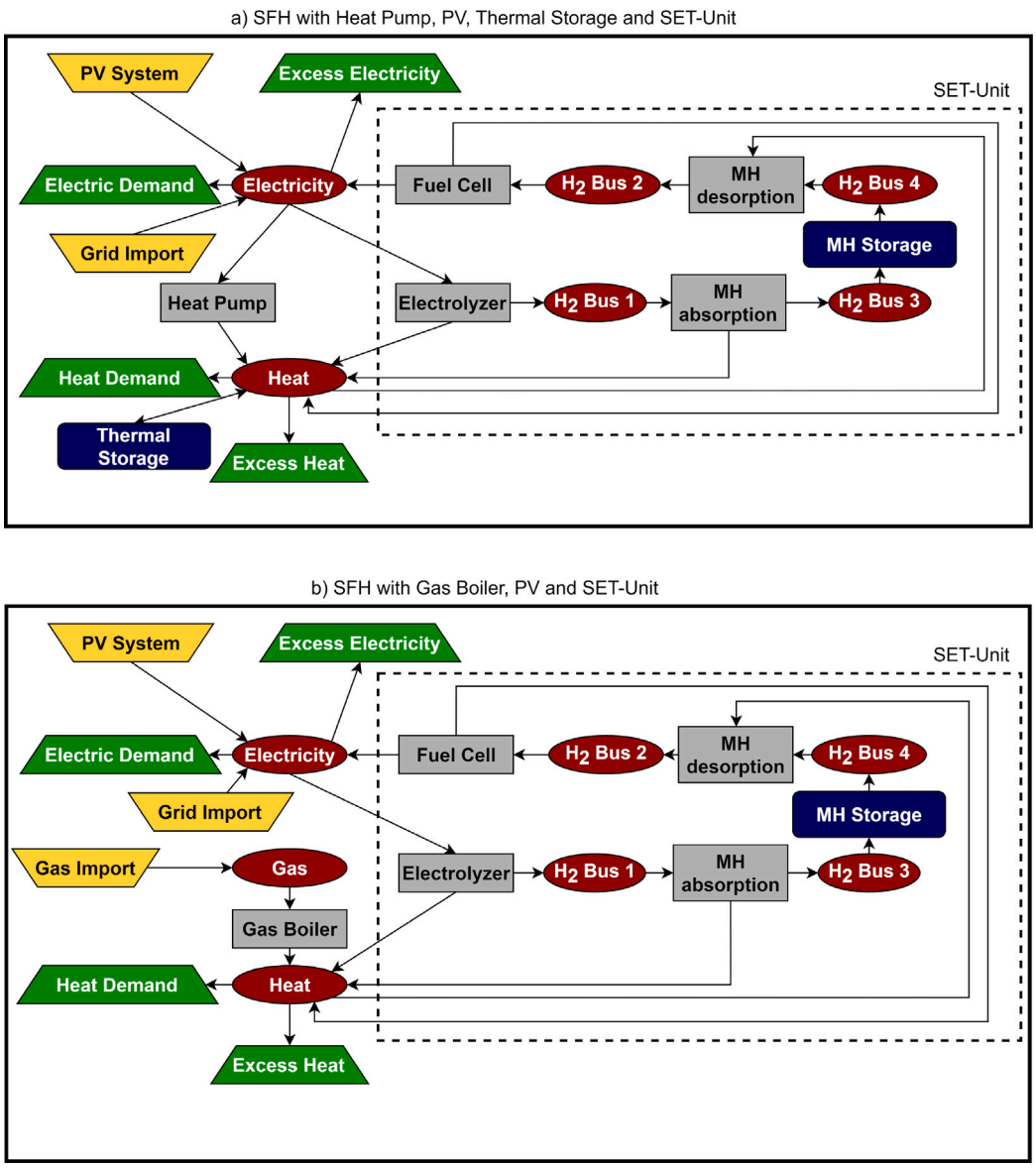

Fig. 3. Energy system model built in oemof for the two types of single-family houses (SFH): (a) SFH with heat pump, PV, thermal storage, and SET-Unit and (b) SFH with gas boiler, PV and SET-Unit.

2.3.1. Electric load profile (ELP)

The annual electric demand in each SFH was assumed to be 4919 kWh as this was the average for a household that had three members or more in Germany in 2019 [36]. From this annual number, the hourly ELP was generated by using the python package demandlib [37] which is part of oemof.

2.3.2. Heat load profile (HLP)

On average, a household with three or more persons in Germany had 16 560 kWh of annual space heating demand and 4842 kWh of hot water demand in 2019 [36], yielding an annual heat demand of 21 402 kWh, which was assumed in this investigation for each SFH. To obtain the hourly HLP, the first step was to define hourly temperature profiles, which were gathered from the Deutscher Wetterdienst (DWD) [38]. The latitude and longitude coordinates that were used are seen in Table 1 for a location in Northern Germany. Then, the hourly temperature profiles, together with the annual heat demand, were given as inputs to the Python package demandlib [37] to generate the hourly HLP.

2.3.3. Electricity price (P_{elec}) and gas price (P_{gas})

The P_{elec} was assumed to be constant for the entire year at a value of 0.4135 EUR/kWh, which was an average household price in 2024 [39]. For the P_{gas}, a value of 0.1068 EUR/kWh was an average value in 2024 for households in Germany [40]. Static prices for gas and electricity were used in the simulation since they are still dominant in Europe. Dynamic prices would increase revenue of any system adding flexibility in a household. In that sense, using static prices is a worst-case scenario for this system.

2.3.4. Hourly PV profile

The Photovoltaic Geographical Information System (PVGIS) tool [41] was employed to obtain the hourly PV profile. This tool can provide hourly PV generation profiles for a PV system with specific parameters, including its geographical coordinates. The list of input parameters assumed for the generation of the hourly PV profile with PVGIS can be seen in Table 1. For the SFH with heat pump, the PV system capacity was assumed to be 10 kW. For the SFH with gas boiler for the case with SET-Unit, 10 kW was assumed as the maximum possible capacity for the optimization in the energy system model.

Table 1
Parameters for the generation of the hourly PV profile. The latitude and longitude were also used to obtain hourly temperature profiles from DWD.

Parameter	Value
Latitude	53.137°
Longitude	8.187°
Database	PVGIS-ERA5
Slope	44°
Azimuth	−9°
System losses	14%
Type of modules	Crystalline Silicon
Maximum size of PV system	10 kW

Table 2
Parameters assumed for the heat pump, gas boiler, thermal storage, PV system and components of the SET-Unit.

Device	Parameters
Heat pump	Rated heat power: 9 kW COP: 3
Gas boiler	Rated heat power: 9 kW Efficiency (gas to heat): 92%
Thermal storage	Height: 1.0 m Diameter: 1.0 m Temperature at hot side: 55 °C Temperature at cold side: 30 °C Temperature outside the storage (fixed): 30 °C
Electrolyzer	Efficiency: 62.5% Usable waste heat: 29.2%
Fuel cell	Efficiency: 45% Usable waste heat: 43%
MH storage	Weight content of hydrogen: 1.6% Heat released in absorption: 0.0896 kWh-heat per kWh of H_2 Heat required in desorption: 0.13248 kWh-heat per kWh of H_2
PV system	Maximum power: 10 kW Feed-in tariff: 0.082 EUR/kWh

2.3.5. Parameters for devices

The assumptions made for each device can be seen in Table 2. This include the parameters for the devices in the household for the reference case, i.e., heat pump, thermal storage and PV for the first type of SFH, and gas boiler for the second type of SFH. It also includes the parameters for the devices of the case with SET-Unit, i.e., electrolyzer, fuel cell, MH storage, and PV system. The usable waste heat from the electrolyzer is the percentage of the maximum electrical power consumption that can be converted to heat during electrolyzer operation. Similarly, the fuel cell's usable waste heat denotes the amount of energy from hydrogen (low heating value) converted to usable heat during fuel cell operation.

2.4. Dispatch optimization

The economic dispatch, i.e., dispatch optimization, of the energy system for each SFH was performed in oemof. This means that the electricity and heat demand of the household were satisfied at the minimum costs. It yielded as output the optimal sizes of the MHS, EL, FC and PV, as well as the hourly electric and heat dispatch of the system. From these time series, annual energy flows were extracted in order to calculate annual costs for the SFH. The energy system model was solved in oemof.solph, a subpackage of oemof, using linear programming (LP), and the solver backend CBC was used. The following Python packages were used: oemof.solph version 0.5.0, oemof.network version 0.5.0a1, oemof.thermal version 0.0.6.dev2 (for modeling the stratified thermal storage and calculating its losses), pandas version 1.5.1, numpy version 1.23.5, pyomo version 6.5.0, and demandlib version 0.1.9.

2.4.1. Total energy cost

Costs for the SFH were calculated as the sum of the products of the variable costs of the sources with the total annual energy of the sources. For the models, variable costs were the electricity price at the grid import source and the gas price at the gas import source (Fig. 3). For the reference case, the total annual energy cost for the SFH with heat pump $C_{hp,ref}$ (in EUR) is:

$$C_{hp,ref} = E_{grid} \cdot P_{elec} - E_{exc} \cdot P_{fit} \quad (1)$$

where E_{grid} is the total annual grid import (in kWh), P_{elec} is the electricity price (in EUR/kWh), E_{exc} is the annual excess electricity (in kWh), P_{fit} is the feed-in tariff for PV (in EUR/kWh). The annual sales of excess electricity at the feed-in tariff price due to the annual excess PV generation offset the variable cost of the system (Fig. 3).

For the SFH with gas boiler, the total annual energy cost $C_{gb,ref}$ (in EUR) is:

$$C_{gb,ref} = E_{grid} \cdot P_{elec} + E_{gas} \cdot P_{gas} \quad (2)$$

where E_{grid} is the total annual grid import (in kWh), P_{elec} is the electricity price (in EUR/kWh), E_{gas} is the total annual gas import (in kWh), and P_{gas} is the gas price (in EUR/kWH).

The total energy cost for a year for the SFH with heat pump for the case with SET-Unit $C_{hp,set}$ (in EUR) is calculated as in the reference case:

$$C_{hp,set} = E_{grid} \cdot P_{elec} - E_{exc} \cdot P_{fit} \quad (3)$$

while for the gas boiler with SET-Unit and PV, the total annual energy cost $C_{gb,set}$ (in EUR) is calculated as:

$$C_{gb,set} = E_{grid} \cdot P_{elec} + E_{gas} \cdot P_{gas} - E_{exc} \cdot P_{fit} \quad (4)$$

2.4.2. Capital expenditures

The capital expenditures $CAPEX$ are the costs related to the investment needed for acquiring a device or technology. The reference case of both SFH has no investments. For the SFH with heat pump for the case with SET-Unit, the total capital expenditure $CAPEX_{total,hp}$ (in EUR) is calculated as the sum of the $CAPEX$ (in EUR) of each device of the SET-Unit:

$$CAPEX_{total,hp} = CAPEX_{ez} \cdot S_{ez} + CAPEX_{fc} \cdot S_{fc} + CAPEX_{mhs} \cdot S_{mhs} \quad (5)$$

And for the SFH with gas boiler for the case with SET-Unit, $CAPEX_{total,gb}$ (in EUR) is:

$$CAPEX_{total,gb} = CAPEX_{ez} \cdot S_{ez} + CAPEX_{fc} \cdot S_{fc} + CAPEX_{mhs} \cdot S_{mhs} + CAPEX_{pv} \cdot S_{pv} \quad (6)$$

where $CAPEX_{ez}$ (in EUR/kW), $CAPEX_{fc}$ (in EUR/kW), $CAPEX_{mhs}$ (in EUR/kg of H_2 storage capacity) and $CAPEX_{pv}$ (in EUR/kW) denote the capital expenditures of the devices: electrolyzer, fuel cell, MH storage and PV system, respectively. Similarly, S_{ez} (in kW), S_{fc} (in kW), S_{mhs} (in kg of H_2 storage capacity) and S_{pv} (in kW) denote the sizes of these devices for each SFH. These sizes were obtained as output from the dispatch optimization.

In literature, a wide range of reported $CAPEX$ values can be found for the subsystems of the SET-Unit. For proton exchange membrane electrolyzers (PEM), alkaline electrolyzers (AEL) and anion exchange membrane electrolyzers (AEM), $CAPEX$ values range from 249 to 3224 EUR/kW [42]. For PEM fuel cells, values range between 422 to 12 669 EUR/kW for the $CAPEX$ [42]. The $CAPEX$ of the MH storage, expressed in EUR/kg of H_2 storage capacity, depends on the type of material employed and the scale of the application. Calculated values include 3158 EUR/kg H_2 for the use of lanthanum pentanickel for heating purposes in a 10-apartment residential building [23], 1182 EUR/kg H_2 for a large-scale hydrogen storage system (5000 tonnes of hydrogen capacity) with lanthanum pentanickel [43], and 3750 EUR/kg H_2 for

Table 3
$CAPEX$ assumptions for the devices of the SET-Unit.

Device	CAPEX
Electrolyzer	249 EUR/kW
Fuel cell	422 EUR/kW
MH storage	1182 EUR per kg of H_2 storage capacity
PV system	1450 EUR/kW

the material cost of titanium iron alloy [35]. The $CAPEX$ for solar rooftop PV systems in Germany is currently between 1450 and 2000 EUR/kW$_p$ for systems up to 10 kW$_p$ [44]. In this study, the minimum $CAPEX$ values found in literature for each device were used and are depicted in Table 3. These values represent favorable economic conditions for the adoption of hydrogen and these technologies.

2.5. Payback period

The payback period is the time that is needed to recover the total cost of an investment made in a technology. For its calculation, the annual savings brought by the SET-Unit were determined first. The annual savings were calculated as the difference between the total annual costs of the reference case with the SET-Unit case. For the SFH with heat pump and SET-Unit, the annual savings S_{hp} (in EUR) are:

$$S_{hp} = C_{hp,ref} - C_{hp,set} \tag{7}$$

Moreover, for the SFH with gas boiler and SET-Unit, the annual savings S_{gb} (in EUR) are:

$$S_{gb} = C_{gb,ref} - C_{gb,set} \tag{8}$$

Then, the payback period PP (in years) considering the $CAPEX$ and the annual savings is calculated for the SFH with heat pump as:

$$PP_{hp} = \frac{CAPEX_{total}}{S_{hp}} \tag{9}$$

while for the SFH with gas boiler, it is:

$$PP_{gb} = \frac{CAPEX_{total}}{S_{gb}} \tag{10}$$

2.6. Self-sufficiency

The self-sufficiency ratio is a quantity that represents the amount of energy demand that is covered by renewable energy. The higher the self-sufficiency ratio, the less the energy imports needed for covering the electricity and heat demands. The self-sufficiency ratio SSR is calculated for the SFH with heat pump as:

$$SSR_{hp} = 100 \cdot \frac{E_{pv} - E_{exc} + (COP - 1) \cdot E_{el,hp}}{E_{elec,dem} + E_{heat,dem}} \tag{11}$$

and for the SFH with gas boiler:

$$SSR_{gb} = 100 \cdot \frac{E_{pv} - E_{exc}}{E_{elec,dem} + E_{heat,dem} + E_{gb} \cdot (1 - \eta_{gb})} \tag{12}$$

where E_{pv} is the annual PV generation (in kWh), $E_{el,hp}$ is the annual electricity consumption by the heat pump (in kWh), $E_{elec,dem}$ is the annual electric demand (in kWh), $E_{heat,dem}$ is the annual heat demand (in kWh), E_{gb} is the annual gas consumption by the gas boiler (in kWh), and η_{gb} is the efficiency of the gas boiler.

3. Results

In this section, the results of the dispatch optimization models for the reference case and the case with SET-Unit are presented. These investigations include the optimal sizes of the EL, FC, MH storage, PV, and the total cost of the system for the case with SET Unit.

Table 4
Optimized capacity for each SFH for the case with SET-Unit.

Device	Capacity for SFH with heat pump	Capacity for SFH with gas boiler
MHS	0.54 kg of hydrogen tank capacity	0.60 kg of hydrogen tank capacity
Electrolyzer	3.29 kW electricity	4.13 kW electricity
Fuel Cell	0.82 kW electricity	0.85 kW electricity
PV system	10 kW (included in reference case)	10 kW

3.1. Dispatch optimization

The sizes of the devices for the case with SET-Unit can be seen in Table 4. These are the optimal sizes that minimize the total system cost, i.e., the total energy cost for a year (Eqs. (3) and (4)) and the total $CAPEX$ (Eqs. (5) and (6)). As the initial SFH with the heat pump already had a PV system of 10 kW, no further size optimization for this component was required. The corresponding weight of the hydride-forming alloy in the MH storage is 34 kg and 38 kg for the SFH with heat pump and for the SFH with gas boiler, respectively.

The monthly electricity and heat energy flows for the SFH with heat pump, thermal storage (TS), and PV can be seen as stacked bar plots in Fig. 4 for the reference case, and in Fig. 5 for the case with SET-Unit. These were obtained by taking the hourly electric and hourly heat dispatch curves (output of the model) and calculating the total energy per month. An inspection was performed on the hourly electricity and heat dispatch curves of the case with SET-Unit to discard either simultaneous MH absorption and desorption, or simultaneous operation of the electrolyzer and fuel cell, and no cases were found. On one hand, energy demands in Figs. 4 and 5 are depicted as positive energy flows, which for the electrical energy include the heat pump, demand, excess PV generation, and electrolyzer. For heat, demands include the heat demand (space heating plus hot water demand), TS charge and desorption process in the MH storage. On the other hand, energy supply can be seen as negative energy flows, which for the electrical energy include the PV, grid import, and fuel cell. For the heat energy, energy supply include the heat pump, TS discharge, electrolyzer, fuel cell and absorption process in the MH storage. The sum of the energy demands is equal to the sum of the energy supply for both the electrical and heat energy flows. The MH storage performed a total of 158 cycles for the entire year.

For both cases, it can be seen in Figs. 4(a) and 5(a) that due to the low PV generation in December, January and February, the monthly amounts of grid import to cover the heat pump and the electrical demand were the highest during these months. The monthly heat supplied by the heat pump was also the highest during these months due to the heat demand, as seen in Figs. 4(b) and 5(b). From March to November, the significant PV generation reduced the amount of electricity imported from the grid for both cases. However, the electrical energy plot for the SET-Unit case shows that the amount of electricity imported was less compared to the reference case. This was due to the operation of the electrolyzer to produce hydrogen and store it in times when there was enough PV generation, and then operating the fuel cell to produce electricity to cover electricity demands. The electricity produced by the fuel cell reduced part of the grid import during March, October and November and almost fully replaced the amount of grid import from April to September. For the SFH with heat pump for the reference case and the case with SET-Unit, the annual grid import E_{grid} was 6756 kWh and 5376 kWh, respectively.

The produced heat during the absorption of hydrogen, as well as during the operation of the electrolyzer and the fuel cell, slightly reduced the amount of heat produced by the heat pump, as seen in Fig. 5(b). The amounts of heat demand during desorption and heat produced during absorption were not significant, however. In addition,

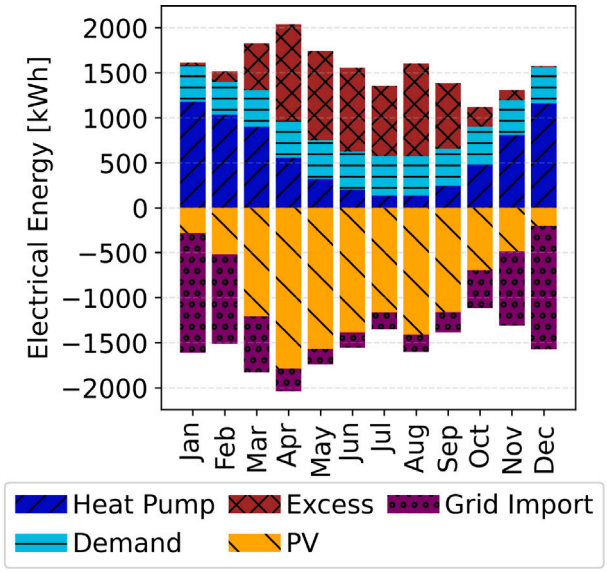

(a) Electrical energy for reference case.

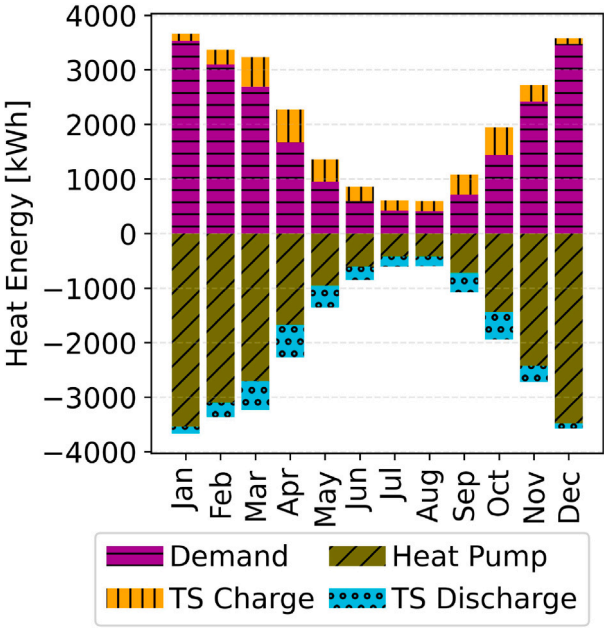

(b) Heat energy for reference case.

Fig. 4. Monthly electricity (a) and heat flows (b) for the SFH with heat pump, thermal storage (TS), and PV for the reference case.

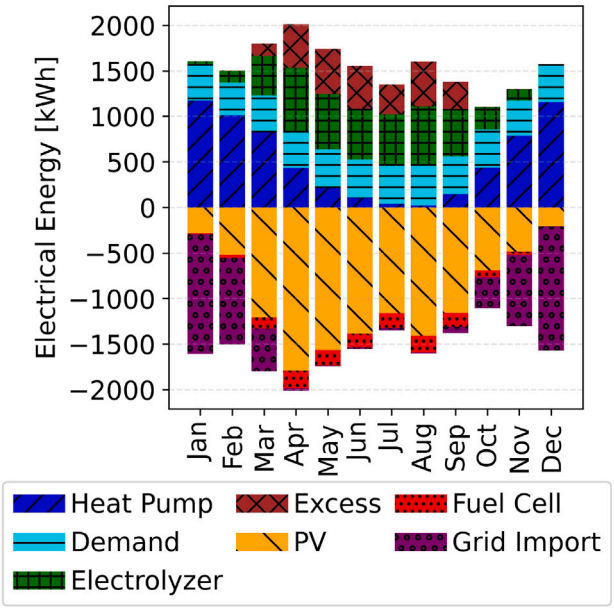

(a) Electrical energy for SET-Unit case.

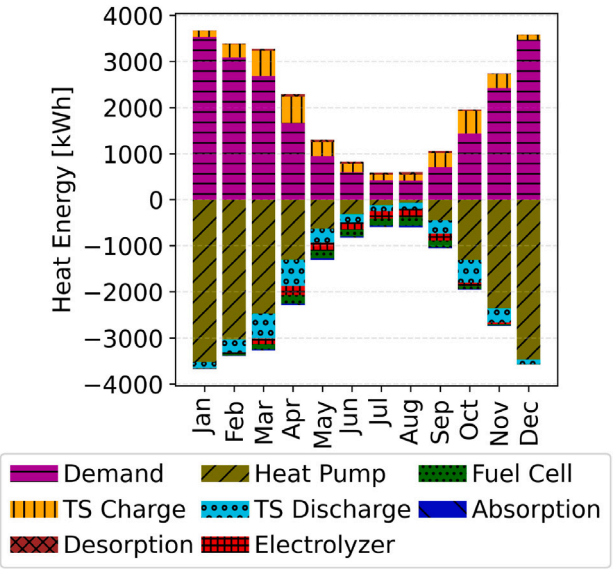

(b) Heat energy for SET-Unit case.

Fig. 5. Monthly electricity (a) and heat flows (b) for the SFH with heat pump, thermal storage (TS), and PV for the case with SET-Unit.

the TS was key in both cases for absorbing heat when it was economically feasible (TS charge) and releasing it when needed (TS discharge), although no noticeable change was seen when comparing both cases. It is also interesting to note that for the SET-Unit case, the amount of excess electricity sold to the grid was less compared to the reference case, as part of the PV generation was used to operate the electrolyzer instead of selling this to the grid.

The monthly electricity and heat energy flows for the SFH with gas boiler can be seen in Fig. 6 for the reference case, and in Fig. 7 for the case with SET-Unit. The aforementioned convention for the energy flows considered as supply or demand is applied here as well. In the reference case, the electricity grid import fully matched the electric demand (Fig. 6(a)), and similarly, all the heat produced by the gas boiler covered the heat demand (Fig. 6(b)). For the case with SET-Unit (Fig. 7(a)), the grid import was reduced by 78%, especially from March to September, due to high PV generation during these months which caused the electrolyzer to operate to store hydrogen and further releasing it to be consumed in the fuel cell for electricity production. In addition, a noticeable amount of excess electricity was sold to the grid during these months. For the SFH with gas boiler for the reference case, the annual gas import E_{gas} was 23 264 kWh and the annual grid import E_{grid} was 4919. The annual gas import was 20 086 kWh and the annual grid import was 1085 kWh for the case with SET-Unit. The MH storage performed 179 cycles for the entire year.

As in the SFH with heat pump, the heat produced mainly from the electrolyzer and fuel cell (Fig. 7(b)) reduced the amount of heat produced from the gas boiler compared to the reference case (Fig. 6(b)), while the amounts of heat during absorption and desorption had small

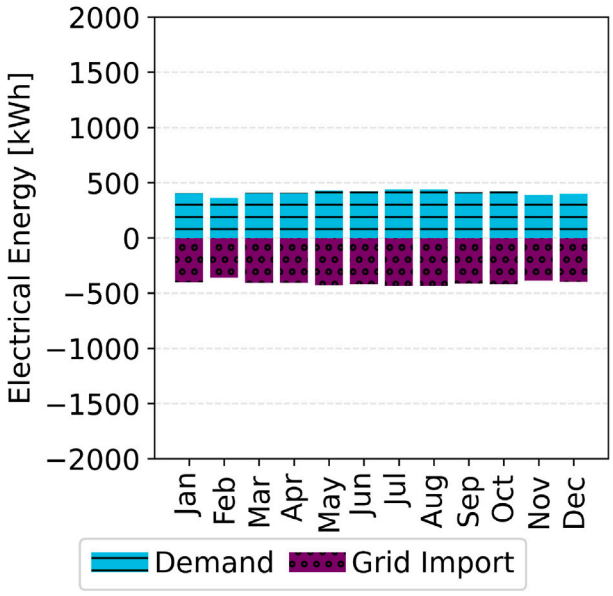

(a) Electrical energy for reference case.

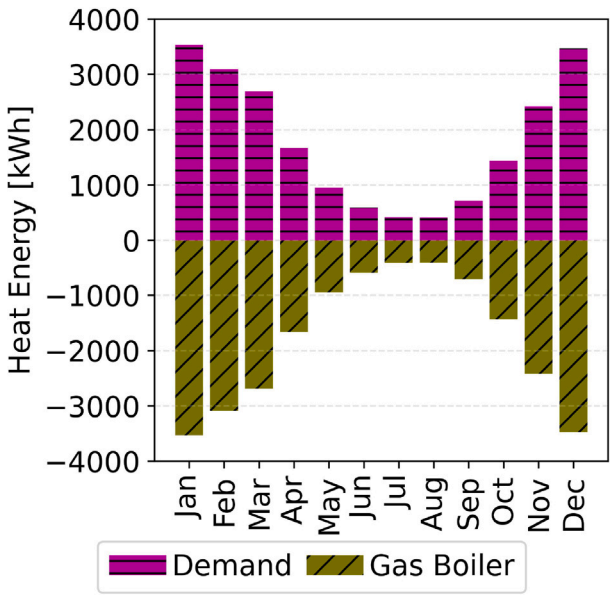

(b) Heat energy for reference case.

Fig. 6. Monthly electricity (a) and heat flows (b) for the SFH with gas boiler for the reference case.

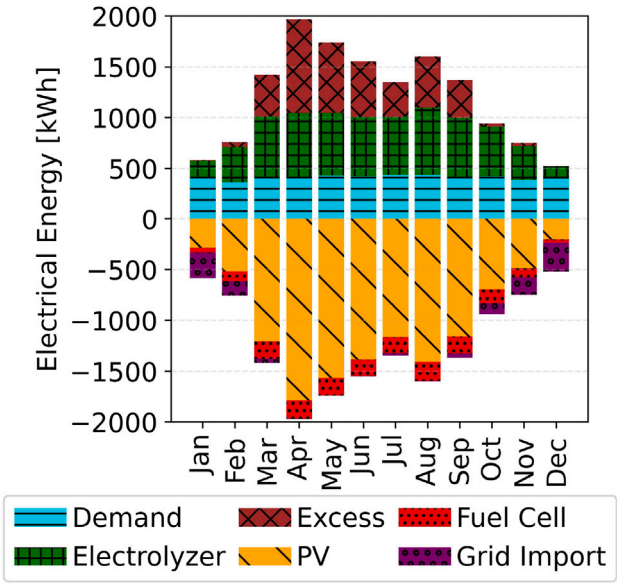

(a) Electrical energy for SET-Unit case.

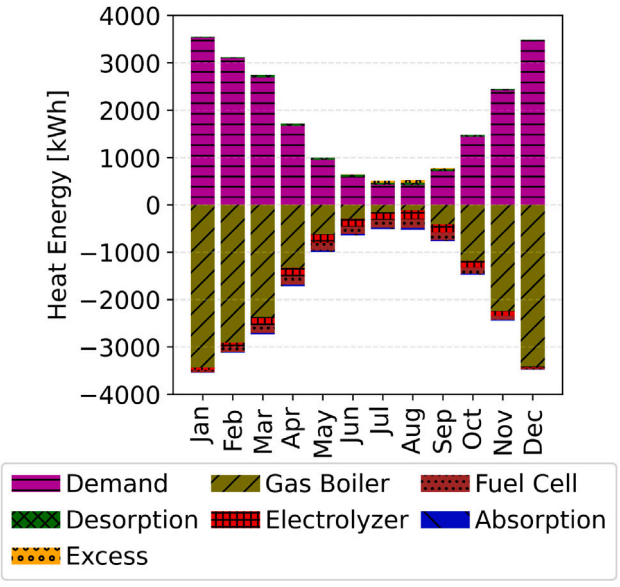

(b) Heat energy for SET-Unit case.

Fig. 7. Monthly electricity (a) and heat flows (b) for the SFH with gas boiler for the case with SET-Unit.

contributions. There was a small amount of excess heat during July and August produced by the electrolyzer and fuel cell which was neither stored nor consumed due to the low heat demand during these months.

3.2. Total energy cost

The annual energy costs and energy sold (Eqs. (1) to (4)) can be seen in Fig. 8. The annual energy sold, i.e., excess electrical energy from PV sold at a FIT price, is displayed on the negative y-axis. The annual cost of importing electricity from the grid (blue), the cost of importing gas from the grid (orange) and the total energy cost are depicted on the positive y-axis. It can be seen that the total energy cost for the SFH with heat pump for the case with SET-Unit is less compared to the case without it, reaching around 2000 EUR. Although the sales of excess PV generation had a reduction of around 315 EUR, the cost of importing electricity got a bigger reduction and reached 571 EUR less. For the SFH with gas boiler, a higher reduction in the cost of importing electricity (around 1585 EUR less) than in the cost of importing gas (around 340 EUR) was seen for the case with SET-Unit compared to the reference case, and approx. 322 EUR was sold as excess PV. These reductions, together with the electricity sold, led to a higher reduction of the total energy cost for the SFH with a gas boiler compared to the SFH with a heat pump that initially had a PV system.

4. Discussion

The annual savings per SFH for the case with SET-Unit and compared to the reference case (Eqs. (7) and (8)) were calculated. Around 255 EUR are saved annually in total energy cost with the SET-Unit

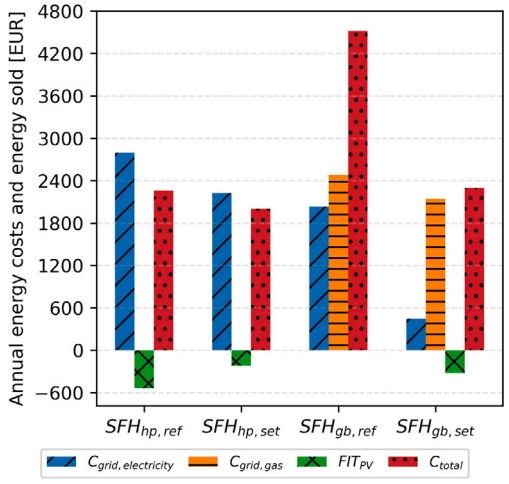

Fig. 8. Energy costs and energy sold for a year. $SFH_{hp,ref}$: house with heat pump for the reference case. $SFH_{hp,set}$: house with heat pump for the case with SET-Unit. $SFH_{gb,ref}$: house with gas boiler for the reference case. $SFH_{gb,set}$: house with gas boiler for the case with SET-Unit. $C_{grid,electricity}$: cost of importing electricity. $C_{grid,gas}$: cost of importing gas. FIT_{PV}: sales of excess PV generation. C_{total}: total energy cost. (For interpretation of the references to colour in this figure legend, the reader is referred to the web version of this article.)

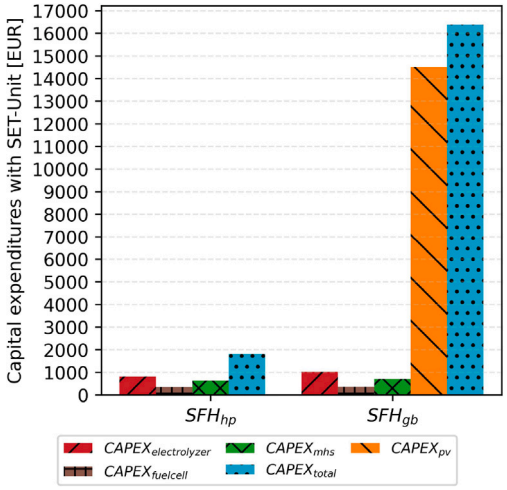

Fig. 9. Capital expenditures for each SFH.

for the SFH with heat pump, thermal storage and PV. The savings are relatively small due to the fact that the route of producing heat to supply the SFH heat demand (much higher than the electricity demand) with the heat pump has a lower cost and higher efficiency (COP of heat pump) than the route of producing heat with the electrolyzer, MH storage and operation of the fuel cell. As a comparison, using 1 kWh of electricity in the heat pump yields 3 kWh of heat. Therefore, the energy cost (disregarding $CAPEX$) to produce 1 kWh of heat with the heat pump is: $1\ \text{kWh},heat \cdot \frac{1\ \text{kWh},elec}{3\ \text{kWh},heat} \cdot \frac{0.41 EUR}{1\ \text{kWh},elec} = 0.13$ EUR. On the other hand, by using the values for the SET-Unit in Table 2, 1 kWh of electricity stored in the SET-Unit and reconverted to electricity and heat yields 1.38 kWh of heat: 1 kWh of electricity consumed by the electrolyzer yields 0.63 kWh of hydrogen, 0.29 kWh of usable heat produced by the electrolyzer, and 0.06 kWh of heat released during the absorption process of the MH storage. Using then the 0.63 kWh of hydrogen stored to operate the fuel cell yields 0.28 kWh of electricity, 0.27 kWh of heat produced by the fuel cell, while 0.08 kWh of heat is required during the desorption process of the MH storage. In addition, the yield of 0.28 kWh of electricity can be converted to 0.84 kWh of heat with the heat pump. So, the total heat produced is: $(0.29 + 0.06 + 0.27 - 0.08 + 0.84)\ \text{kWh},\text{heat} = 1.38\ \text{kWh},\text{heat}$, and the energy cost is: $1\ \text{kWh},heat \cdot \frac{1\ \text{kWh},elec}{1.38\ \text{kWh},heat} \frac{0.41 EUR}{1\ \text{kWh},elec} = 0.30$ EUR. The energy cost of producing heat with the heat pump is lower than with the SET-Unit. Therefore, adding the SET-Unit to the initial SFH did not make a huge impact in economic savings. However, having the possibility of storing PV electricity as hydrogen in the MH storage instead of selling it as excess FIT and using it when needed played a role in reducing the total annual grid import costs.

A bigger saving of the total energy cost of around 2221 EUR was seen with the SET-Unit for the SFH with gas boiler. The energy cost to produce 1 kWh of heat with the gas boiler is: $1\ \text{kWh},heat \cdot \frac{1\ \text{kWh},gas}{0.92\ \text{kWh},heat} \cdot \frac{0.11 EUR}{1\ \text{kWh},gas} = 0.12$ EUR. To calculate the energy cost to produce 1 kWh of heat with the SET-Unit, the same calculations are done as described previously in the case of the SET-Unit with heat pump but now with an exclusion. This is to exclude the amount of heat produced by the heat pump with the electricity yield by the fuel cell, i.e., 0.84 kWh of heat, as now there is a gas boiler instead. Then, the total heat produced with 1 kWh of electricity stored and reconverted in the SET-Unit is 0.53395 kWh, and the energy cost is: $1\ \text{kWh},heat \cdot \frac{1\ \text{kWh},elec}{0.53\ \text{kWh},heat} \frac{0.41 EUR}{1\ \text{kWh},elec} = 0.77$ EUR. As seen, the energy cost to produce 1 kWh of heat with the gas boiler is lower than with the SET-Unit. However, as the reference SFH with gas boiler did not have a PV system, adding it together with the SET-Unit significantly reduced the total energy costs, as part of the PV generation was sold as FIT and another portion was shifted via storage in the SET-Unit for later demand satisfaction.

For the SFH with gas boiler for the case with SET-Unit, it was further investigated what were the individual contributions of the PV system and the SET-Unit in the total energy cost of the system, as the reference case did not contemplate a PV system for the SFH with gas boiler. For this purpose, an additional case of SFH with gas boiler, PV system, and without SET-Unit was modeled, which can be found in Fig. A.10 in the Appendix. In comparison with the SFH with gas boiler for the reference case, it was found that installing the PV system played the biggest role in reducing the total energy cost (1711 EUR reduction), followed by the SET-Unit (510 EUR).

The $CAPEX$ of each device and $CAPEX_{total}$, Eqs. (5) and (6) calculated with the sizes obtained in Table 4, can be seen in Fig. 9. For the SFH with heat pump and SET-Unit, the most relevant contributor to the $CAPEX$ is the electrolyzer (45%), followed by the MH storage (35%) and fuel cell (20%). The PV system has the highest $CAPEX$ of all components and accounted for most of the $CAPEX_{total}$ for the SFH with gas boiler and SET-Unit (88%) followed by the electrolyzer (6%), MH storage (4%) and fuel cell (2%).

The calculated payback period (Eqs. (9) and (10)) for the SFH with gas boiler and SET-Unit is around 7.4 years, and for the SFH with heat pump and SET-Unit it is 7.1 years. Although a higher saving with SET-Unit was observed for the SFH with gas boiler than for the SFH with heat pump, the significantly higher $CAPEX_{total}$ led to a slightly higher payback period. The use of the minimum CAPEX values found in literature for the electrolyzer, fuel cell, metal hydride storage, and PV system (Section 2.4.2) led to a feasible investment in the SET-Unit for the SFHs with gas boiler and heat pump, as there were annual savings and payback periods lower than 10 years. However, it should be noted that the use of average or higher-end CAPEX values reported in literature was excluded from this investigation, because the goal of this study was to demonstrate feasibility. Optimistic CAPEX values reflect a scenario where low investment costs are achieved due to economies of scale. Therefore, it shows the relevant values after the early adoption phase, which is often accompanied by state subsidies in any case. See economics of PV pricing in Germany for comparison [45].

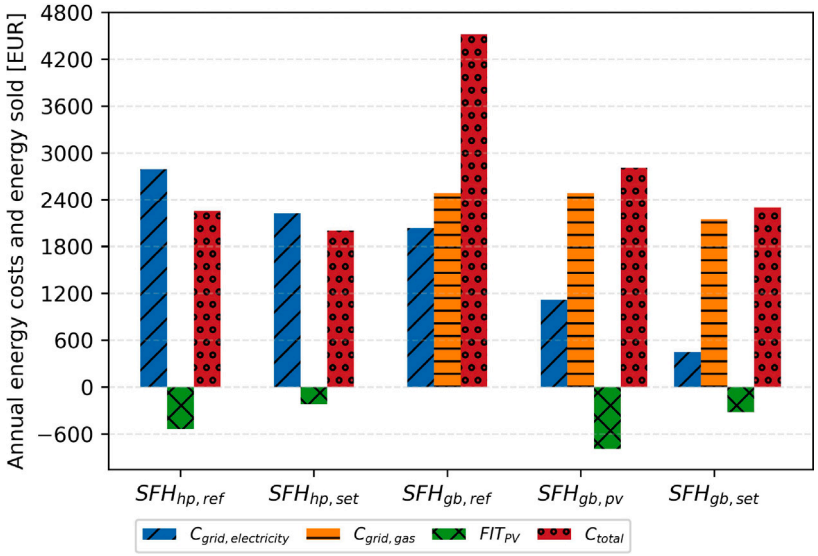

Fig. A.10. Energy costs and energy sold for a year. $SFH_{hp,ref}$: house with heat pump for the reference case. $SFH_{hp,set}$: house with heat pump for the case with SET-Unit. $SFH_{gb,ref}$: house with gas boiler for the reference case. $SFH_{gb,pv}$: house with gas boiler, PV system, and without SET-Unit. $SFH_{gb,set}$: house with gas boiler, PV system, and with SET-Unit. $C_{grid,electricity}$: cost of importing electricity. $C_{grid,gas}$: cost of importing gas. FIT_{PV}: sales of excess PV generation. C_{total}: total energy cost.

Table 5
Self-sufficiency of each SFH for each case.

Type of SFH	Case	Self-sufficiency
Heat pump, thermal storage and PV	Reference	75%
	SET-Unit	83%
Gas boiler	Reference	0%
	SET-Unit with PV	28%

The self-sufficiency values (Eqs. (11) and (12)) for both SFH are depicted in Table 5. Because of the reduced electricity import from the grid E_{grid} due to the PV system and the MH storage, the self sufficiency for the SFH with heat pump is higher than without the SET-Unit. For the SFH with gas boiler for the reference case, all the electricity demand was supplied by E_{grid}, therefore there is no self sufficiency. With respect to the gas boiler for the case with SET-Unit and PV, a lower value was observed than with the SFH with the heat pump. This is due to the high annual gas import E_{gas} needed for the gas boiler to satisfy the heat demand, in comparison with the lower E_{grid} needed for the heat pump to provide heat. It should be noted that the dispatch optimization model did not aim to maximize the self-sufficiency of the system even though the optimization goal was to minimize the total energy cost for a year and the total $CAPEX$.

As reported in Table 4, the optimized capacities range between 0.54 and 0.60 kg of hydrogen. Such a tank size offers flexibility and faster kinetic behavior than larger tanks. Kaoutari et al. [46] investigated the integration of a 0.75 kW PEM fuel cell micro-combined heat and power system with MH hydrogen storage for a 120 m^2 residential application. Applying genetic algorithm optimization identified an optimal metal hydride tank size of 6500 NL (i.e., 0.58 kg), covering approximately 68% of the hydrogen gas consumption and 65% of the production for the residential system. Therefore, for households, the here-identified optimal metal hydride tank size agrees with what has already been reported in the literature for the same application.

In the field of energy storage, a MH storage system, in comparison with battery storage technologies, has advantages and disadvantages. A battery system has a clear advantage in terms of round trip efficiency: Using the values in Table 2, and using 90% as the inverter efficiency, a MH storage system has a round trip efficiency of 81% using all of the waste heat and 25% otherwise compared to 85% of a battery system [47]. In addition, even using the waste heat is less efficient in comparison to a battery system because if a heat pump is present in both systems, any electricity to (usable) waste heat conversion is missing the COP boost of the heat pump. These values are included in the dispatch simulation since it impacts the cost of stored energy to produce heat (see Section 4). Storing energy in the MH storage is relatively easy. Fast hydrogen refueling can be mentioned. Another important feature of the metal hydride tanks is proven cycling stability of 2000 cycles with less than 5% hydrogen capacity loss, using materials similar to the room-temperature hydrides proposed here [48]. Moreover, similar room-temperature hydrides have shown good stability over 20,000 cycles, with a capacity reduction of about 25%, which can be regenerated under relatively high-temperature (380 °C) and vacuum conditions [49]. In this work, the MH storage performs 158 and 176 cycles a year, which is far less than the tested cycles. Comparing that to a battery system, which has a cycle life of 2000 cycles or 7 years depending on temperature, used C-rate and chemistry to name a few related factors [50], shows an advantage of the MH storage system in terms of stability. In addition, the output of the hydrogen storage system (kW) is independent of the capacity (kWh): with battery storage, the charge and discharge power is limited by the capacity, but for the hydrogen storage system, the charge and discharge rates do not depend solely on the capacity of the tank. For long-term storage, the battery has to be relatively large so that the discharge power satisfies the power demand, although the full capacity might not be required, and having the battery fully charged for longer periods degrades it. In contrast, MH storage can store energy for long periods of time without time dependent losses. However, there are also disadvantages of MH storage in comparison with battery storage. Operating the MH storage involves a complex heat management system with heat losses in the system, and an adequate sizing of a heat exchanger is necessary for absorbing heat and providing heat for the absorption and desorption of hydrogen, respectively. In addition, the heat required to desorb the hydrogen might be higher than the amount of heat released to absorb the hydrogen, which results in a net heat required for the system. No rigorous heat exchanger is typically needed for battery storage when compared to the SET-Unit heat exchange requirements. Nonetheless, for certain applications, such as backup power and long-term storage, MH storage is a more volumetric efficient solution than battery storage. A relevant aspect of the MH storage system is reducing the CO2 footprint.

Puszkiel et al. [35] investigated the global warming potential (GWP in kg CO2eq/kg H2) of the MH storage system. It was found that the use of a recycled hydride-forming alloy reduces the material's GWP by 79.8%. Furthermore, the heat required for the dehydrogenation process significantly influences the GWP of the MH storage system. The use of recoverable heat, as proposed in this work, reduces the system's GWP impact by about a factor of 10 compared with energy from the electric grid or natural gas.

5. Conclusions

This paper presents the design and operation of a coupled renewable energy system for simultaneous electricity and heat supply, aiming to minimize costs. A simulation framework in Python (oemof) was developed to analyze the Smart-Energy-Transform-Unit, SET-Unit (EL-FC-MH) from the Digi-HyPro project. The strategic storage of photovoltaic (PV) electricity as hydrogen in metal hydride (MH) storage systems has been demonstrated to be a cost-effective approach to reduce grid import expenses. The system, which incorporates a heat pump, PV technology, thermal storage, and a SET-Unit, achieves 83% self-sufficiency, reducing annual energy expenditures by 255 EUR and providing a 7.1-year payback period. The electrolyzer (45%), the MH storage (35%), and the fuel cell (20%) are the primary contributors to the capital expenditures. Conversely, a system employing a gas boiler, PV technology, and a SET-Unit attains 28% self-sufficiency, thereby reducing annual expenditures by 2221 EUR and attaining a payback period of 7.4 years. In this configuration, the PV system accounts for 88% of the capital expenditure (CAPEX), followed by the electrolyzer (6%), MH storage (4%), and fuel cell (2%). For future research on the topic, the degradation of the main components of the SET-Unit, such as the electrolyzer and fuel cell, the dynamic changes in electricity prices and gas prices, and the modeling of the thermodynamic and kinetics behavior of the MH material including its thermal conductivity, are to be considered.

CRediT authorship contribution statement

Carlos Muñoz: Writing – original draft, Visualization, Software, Methodology, Investigation, Formal analysis, Conceptualization. **Nies Reininghaus:** Writing – review & editing, Supervision, Resources, Methodology, Conceptualization. **Julián Puszkiel:** Writing – review & editing, Project administration, Conceptualization. **Astrid Pistoor:** Writing – review & editing, Conceptualization. **Michael Kroener:** Writing – review & editing, Supervision. **Alexander Dyck:** Supervision. **Martin Vehse:** Supervision. **Thomas Klassen:** Project administration, Funding acquisition. **Julian Jepsen:** Project administration, Funding acquisition.

Declaration of competing interest

The authors declare that they have no known competing financial interests or personal relationships that could have appeared to influence the work reported in this paper.

Acknowledgments

This research paper is funded by dtec.bw – Digitalization and Technology Research Center of the Bundeswehr which we gratefully acknowledge. dtec.bw is funded by the European Union – NextGenerationEU.

Appendix. Energy costs

For the SFH with gas boiler for the case with SET-Unit, it was further investigated what were the individual contributions of the PV system and the SET-Unit in the total energy cost of the system, as the reference case did not contemplate a PV system for the SFH with gas boiler. For this purpose, an additional case of SFH with gas boiler, PV system, and without SET-Unit was modeled, which can be found in Fig. A.10 in the Appendix. In comparison with the SFH with gas boiler for the reference case, it was found that installing the PV system played the biggest role in reducing the total energy cost (1711 EUR reduction), followed by the SET-Unit (510 EUR).

Data availability

Data will be made available on request.

References

[1] Barkanov E, Penalba M, Martinez A, Martinez-Perurena A, Zarketa-Astigarraga A, Iglesias G. Evolution of the European offshore renewable energy resource under multiple climate change scenarios and forecasting horizons via CMIP6. Energy Convers Manage 2024;301:118058. http://dx.doi.org/10.1016/j.enconman.2023.118058.

[2] IEA. World energy outlook. 2023, URL https://www.iea.org/reports/world-energy-outlook-2023.

[3] Ahmad S, Ullah A, Samreen A, Qasim M, Nawaz K, Ahmad W, Alnaser A, Kannan AM, Egilmez M. Hydrogen production, storage, transportation and utilization for energy sector: A current status review. J Energy Storage 2024;101:113733. http://dx.doi.org/10.1016/j.est.2024.113733, URL https://www.sciencedirect.com/science/article/pii/S2352152X2403319X.

[4] Shoaei M, Noorollahi Y, Hajinezhad A, Moosavian SF. A review of the applications of artificial intelligence in renewable energy systems: An approach-based study. Energy Convers Manage 2024;306:118207. http://dx.doi.org/10.1016/j.enconman.2024.118207.

[5] United Nations. Progress towards the sustainable development goals: Report of the secretary-general. 2024, URL https://unstats.un.org/sdgs/files/report/2024/SG-SDG-Progress-Report-2024-advanced-unedited-version.pdf.

[6] Faghih A, Roozbehani M, Dahleh MA. On the value and price-responsiveness of ramp-constrained storage. Energy Convers Manage 2013;76:472–82. http://dx.doi.org/10.1016/j.enconman.2013.07.072, URL https://linkinghub.elsevier.com/retrieve/pii/S0196890413004433.

[7] Zhang Z, Yin Z, Yixi J, Zhang Y, Zhu R. A distributionally robust optimization strategy for electric-thermal complementary systems considering joint peaking of thermal power units and pumped-storage hydroelectric units. Sustain Energy, Grids Networks 2025;44:102015. http://dx.doi.org/10.1016/j.segan.2025.102015, URL https://linkinghub.elsevier.com/retrieve/pii/S2352467725003972.

[8] Miskan SN, Abdulkadir BA, Setiabudi HD. Materials on the frontier: A review on groundbreaking solutions for hydrogen storage applications. Chem Phys Impact 2025;10:100862. http://dx.doi.org/10.1016/j.chphi.2025.100862, URL https://linkinghub.elsevier.com/retrieve/pii/S2667022425000507.

[9] Jolly SS, Twinkle A, Arun Sasi B, Reshma R. Emerging paradigms in renewable hydrogen production: Technology challenges, and global impact. Next Energy 2025;8:100343. http://dx.doi.org/10.1016/j.nxener.2025.100343, URL https://linkinghub.elsevier.com/retrieve/pii/S2949821X25001061.

[10] Lange J, Schulthoff M, Puszkiel J, Sens L, Jepsen J, Klassen T, Kaltschmitt M. Aboveground hydrogen storage – assessment of the potential market relevance in a carbon-neutral European energy system. Energy Convers Manage 2024;306:118292. http://dx.doi.org/10.1016/j.enconman.2024.118292.

[11] Chaudhry AK, Sachdeva P. Exploring the capabilities of solid-state systems as a means of storing hydrogen. In: Renewable hydrogen. Elsevier; 2024, p. 107–36. http://dx.doi.org/10.1016/B978-0-323-95379-5.00009-2, URL https://linkinghub.elsevier.com/retrieve/pii/B9780323953795000092.

[12] Yartys VA, Lototskyy MV, Tolj I, von Colbe JB, Denys RV, Davids MW, Nyamsi SN, Swanepoel D, Berezovets VV, Zavaliy I, Suwarno S, Puszkiel IJ, Jepsen J, Ferreira I, Pistidda C, Shang Y, Pasupathi S, Linkov V. HYDRIDE4MOBILITY: An EU project on hydrogen powered forklift using metal hydrides for hydrogen storage and H2 compression. J Energy Storage 2025;109:115192. http://dx.doi.org/10.1016/J.EST.2024.115192.

[13] Bellosta von Colbe J, Ares J-R, Barale J, Baricco M, Buckley C, Capurso G, Gallandat N, Grant DM, Guzik MN, Jacob I, Jensen EH, Jensen T, Jepsen J, Klassen T, Lototskyy MV, Manickam K, Montone A, Puszkiel J, Sartori S, Sheppard DA, Stuart A, Walker G, Webb CJ, Yang H, Yartys V, Züttel A, Dornheim M. Application of hydrides in hydrogen storage and compression: Achievements, outlook and perspectives. Int J Hydrog Energy 2019;44(15):7780–808. http://dx.doi.org/10.1016/J.IJHYDENE.2019.01.104.

[14] Dresden FI. Applications of metal hydrides: Comparison of volumetric hydrogen storage densities. 2024, URL https://www.ifam.fraunhofer.de/en/Aboutus/Locations/Dresden/HydrogenTechnology/hydrides/applications-of-metal-hydrides.html.

[15] Valverde L, Pino FJ, Guerra J, Rosa F. Definition, analysis and experimental investigation of operation modes in hydrogen-renewable-based power plants incorporating hybrid energy storage. Energy Convers Manage 2016;113:290–311. http://dx.doi.org/10.1016/j.enconman.2016.01.036.

[16] Valverde L, Rosa F, Del Real AJ, Arce A, Bordons C. Modeling, simulation and experimental set-up of a renewable hydrogen-based domestic microgrid. Int J Hydrog Energy 2013;38(27):11672–84. http://dx.doi.org/10.1016/j.ijhydene.2013.06.113.

[17] Valverde L, Rosa F, Bordons C, Guerra J. Energy management strategies in hydrogen smart-grids: A laboratory experience. Int J Hydrog Energy 2016;41(31):13715–25. http://dx.doi.org/10.1016/j.ijhydene.2016.05.279.

[18] Ancona M, Bianchi M, Branchini L, De Pascale A, Melino F, Peretto A, Rosati J, Scarponi L. From solar to hydrogen: Preliminary experimental investigation on a small scale facility. Int J Hydrog Energy 2017;42(33):20979–93. http://dx.doi.org/10.1016/j.ijhydene.2017.06.141, URL https://linkinghub.elsevier.com/retrieve/pii/S0360319917324965.

[19] Khayrullina AG, Blinov D, Borzenko V. Novel kW scale hydrogen energy storage system utilizing fuel cell exhaust air for hydrogen desorption process from metal hydride reactor. Energy 2019;183:1244–52. http://dx.doi.org/10.1016/j.energy.2019.07.021, URL https://linkinghub.elsevier.com/retrieve/pii/S0360544219313489.

[20] Endo N, Shimoda E, Goshome K, Yamane T, Nozu T, Maeda T. Construction and operation of hydrogen energy utilization system for a zero emission building. Int J Hydrog Energy 2019;44(29):14596–604. http://dx.doi.org/10.1016/j.ijhydene.2019.04.107, URL https://linkinghub.elsevier.com/retrieve/pii/S0360319919315368.

[21] Zhang Z, Sato K, Nagasaki Y, Tsuda M, Miyagi D, Komagome T, Tsukada K, Hamajima T, Ishii Y, Yonekura D. Continuous operation in an electric and hydrogen hybrid energy storage system for renewable power generation and autonomous emergency power supply. Int J Hydrog Energy 2019;44(41):23384–95. http://dx.doi.org/10.1016/j.ijhydene.2019.07.028, URL https://linkinghub.elsevier.com/retrieve/pii/S0360319919325765.

[22] Parida A, Kumar A, Muthukumar P, Dalal A. Experimental and numerical investigations on synergistic coupling of metal hydride hydrogen storage systems with low-temperature proton exchange membrane fuel-cell. Therm Sci Eng Prog 2024;51:102620. http://dx.doi.org/10.1016/j.tsep.2024.102620, URL https://linkinghub.elsevier.com/retrieve/pii/S2451904924002385.

[23] Esposito L, van der Wiel M, Acar C. Hydrogen storage solutions for residential heating: A thermodynamic and economic analysis with scale-up potential. Int J Hydrog Energy 2024;79:579–93. http://dx.doi.org/10.1016/j.ijhydene.2024.06.279.

[24] dtecbw - Zentrum für Digitalisierungs- und Technologieforschung der Bundeswehr. Digi-HyPro – digitalisierte wasserstoffprozesskette für die energiewende. 2020, URL https://dtecbw.de/home/forschung/hsu/projekt-digi-hypro.

[25] Puszkiel J, Covarrubias Guraneros M, Fleming L, Kaufmann TFJ, Krause P, Warfsmann JH, Wienken ES, Wildner L, Schulze M, Klassen T, Jepsen J, Kutzner H, Gizer G, Bellosta von Colbe, José María, Taube K, Hamedi H, Brinkmann T. Hydrogen in stationary applications: Coupling the electricity, gas and mobility sectors (digi-hypro). 2022, http://dx.doi.org/10.24405/14527.

[26] Puszkiel J, Brinkmann T, Covarrubias M, Fleming L, Höne M, Kaufmann T, Krause P, Warfsmann JH, Wienken ES, Wildner L, Wolf T, Klassen T, Jepsen J, Lange J, Kaltschmitt M, Reininghaus N, Pistoor A, Muñoz Robinson C, Kröner M, Dyck A. Experimental development of the set-unit concept on a laboratory scale for the H_2-chain: Production-storage-compression-utilization (digi-hypro). 2024, http://dx.doi.org/10.24405/16774.

[27] Muñoz Robinson C, Reininghaus N, Pistoor A, Kröner M, Dyck A, Vehse M, Lange J, Kaltschmitt M, Puszkiel J, Covarrubias M, Fleming L, Kaufmann T, Krause P, Warfsmann JH, Wienken ES, Wildner L, Klassen T, Jepsen J. Dispatch optimization of the electricity and heat of the smart-energy-transform-unit. 2024, http://dx.doi.org/10.24405/16775.

[28] Hayn M, Bertsch V, Fichtner W. Electricity load profiles in europe: The importance of household segmentation. Energy Res Soc Sci 2014;3:30–45. http://dx.doi.org/10.1016/j.erss.2014.07.002, URL https://www.sciencedirect.com/science/article/pii/S2214629614000802.

[29] Statistisches Bundesamt. Familien und familienmitglieder nach bundesländern. 2023, URL https://www.destatis.de/DE/Themen/Gesellschaft-Umwelt/Bevoelkerung/Haushalte-Familien/Tabellen/2-3-familien-bundeslaender.html.

[30] BDEW Bundesverband der Energie- und Wasserwirtschaft eV. Wie heizt deutschland? (2023): Studie zum heizungsmarkt. 2023.

[31] Hilpert S, Kaldemeyer C, Krien U, Günther S, Wingenbach C, Plessmann G. The open energy modelling framework (oemof) - a new approach to facilitate open science in energy system modelling. Energy Strat Rev 2018;22:16–25. http://dx.doi.org/10.1016/j.esr.2018.07.001, URL https://www.sciencedirect.com/science/article/pii/S2211467X18300609.

[32] Krien U, Schönfeldt P, Launer J, Hilpert S, Kaldemeyer C, Pleßmann G. Oemof.solph—A model generator for linear and mixed-integer linear optimisation of energy systems. Softw Impacts 2020;6:100028. http://dx.doi.org/10.1016/j.simpa.2020.100028.

[33] Telle J-S, Schlüters S, Schönfeldt P, Hanke B, von Maydell K, Agert C. The optimized integration of temperature-controlled transports into distributed sector-integrated energy systems. Energy Convers Manage 2022;269:116148. http://dx.doi.org/10.1016/j.enconman.2022.116148, URL https://www.sciencedirect.com/science/article/pii/S0196890422009311.

[34] Tiedemann T, Dasenbrock J, Kroener M, Satola B, Reininghaus N, Schneider T, Vehse M, Schier M, Siefkes T, Agert C. Supplying electricity and heat to low-energy residential buildings by experimentally integrating a fuel cell electric vehicle with a docking station prototype. Appl Energy 2024;362:122525. http://dx.doi.org/10.1016/j.apenergy.2023.122525.

[35] Puszkiel J, Neves A, Warfsmann J, Krause P, Kaufmann T, Hoberg AR, Hegen O, Kötter A, Klassen T, Jepsen J. On the hydrogen storage properties and life cycle evaluation of a room temperature hydride for scale-up applications: The case of an AB2-alloy. Int J Hydrog Energy 2025;118:482–99. http://dx.doi.org/10.1016/j.ijhydene.2025.03.161, URL https://www.sciencedirect.com/science/article/pii/S0360319925012753.

[36] Statistisches Bundesamt. Umweltökonomische gesamtrechnungen: Private haushalte und umwelt. 2019, URL https://www.statistischebibliothek.de/mir/receive/DEHeft_mods_00147407.

[37] Krien U. Demandlib documentation. 2024, URL https://demandlib.readthedocs.io/_/downloads/en/stable/pdf/.

[38] Der Deutsche Wetterdienst. Testreferenzjahre (TRY). 2022, URL https://www.dwd.de/DE/leistungen/testreferenzjahre/testreferenzjahre.html.

[39] der Energie-und Wasserwirtschaft e.V. BB. BDEW-strompreisanalyse juli 2024: Haushalte und industrie. 2024, URL https://www.bdew.de/media/documents/240703_BDEW-Strompreisanalyse_Juli_2024_Korrektur.pdf.

[40] der Energie-und Wasserwirtschaft e.V. BB. BDEW-gaspreisanalyse januar 2021: Haushalte. 2024, URL https://www.bdew.de/media/documents/BDEW-Gaspreisanalyse_08-2024.pdf.

[41] Huld T, Müller R, Gambardella A. A new solar radiation database for estimating PV performance in europe and africa. Sol Energy 2012;86(6):1803–15. http://dx.doi.org/10.1016/j.solener.2012.03.006.

[42] Rozzi E, Minuto FD, Lanzini A. Techno-economic dataset for hydrogen storage-based microgrids. Data Brief 2024;56:110795. http://dx.doi.org/10.1016/j.dib.2024.110795, URL https://www.sciencedirect.com/science/article/pii/S2352340924007595.

[43] Abdin Z, Khalilpour K, Catchpole K. Projecting the levelized cost of large scale hydrogen storage for stationary applications. Energy Convers Manage 2022;270:116241. http://dx.doi.org/10.1016/j.enconman.2022.116241, URL https://www.sciencedirect.com/science/article/pii/S0196890422010184.

[44] Fraunhofer ISE, PSE Projects GmbH. Photovolatics report. 2024, URL https://www.ise.fraunhofer.de/content/dam/ise/de/documents/publications/studies/Photovoltaics-Report.pdf.

[45] Benhmad F, Percebois J. Photovoltaic and wind power feed-in impact on electricity prices: The case of Germany. Energy Policy 2018;119:317–26. http://dx.doi.org/10.1016/j.enpol.2018.04.042, URL https://www.sciencedirect.com/science/article/pii/S0301421518302581.

[46] Kaoutari T, Louahlia H, Schaetzel P. Optimization of hydrogen gas storage in PEM fuel cell mCHP system for residential applications using numerical and machine learning modeling. Energy Convers Manage 2025;341:120017. http://dx.doi.org/10.1016/j.enconman.2025.120017, URL https://linkinghub.elsevier.com/retrieve/pii/S0196890425005412.

[47] Rao KD, Reddy KK, Koushik P, Avinash B, Madhavi DL. Performance analysis of lithium-ion battery considering round trip efficiency. In: 2023 IEEE 2nd international conference on industrial electronics: developments & applications (iCIDeA). 2023, p. 555–9. http://dx.doi.org/10.1109/ICIDeA59866.2023.10295170.

[48] Fiori C, Dell'Era A, Zuccari F, Santiangeli A, D'Orazio A, Orecchini F. Hydrides for submarine applications: Overview and identification of optimal alloys for air independent propulsion maximization. Int J Hydrog Energy 2015;40(35):11879–89. http://dx.doi.org/10.1016/j.ijhydene.2015.02.105, URL https://linkinghub.elsevier.com/retrieve/pii/S0360319915005066.

[49] Sandrock G. State-of-the-art review of hydrogen storage in reversible metal hydrides for military fuel cell applications. 1997, URL https://apps.dtic.mil/sti/citations/ADA328073 publisher: Defense Technical Information Center (DTIC).

[50] Zhang J, Huang H, Zhang G, Dai Z, Wen Y, Jiang L. Cycle life studies of lithium-ion power batteries for electric vehicles: A review. J Energy Storage 2024;93:112231. http://dx.doi.org/10.1016/j.est.2024.112231, URL https://www.sciencedirect.com/science/article/pii/S2352152X24018176.